Hardware Design of a Integrated Modular Motor Drive (IMMD)

by

Adam Shea

A thesis submitted in partial fulfillment of
the requirements for the degree of

Master of Science

(Electrical Engineering)

at the

UNIVERSITY OF WISCONSIN–MADISON

November 24, 2014

Contents

List of Figures

Chapter 1

Introduction

The increasing proliferation and maturation of electric drive technologies has caused drive system-level integration to become a high priority in a variety of application areas including electric propulsion, aerospace, white goods, and down-hole drilling. Tight integration of motor and drive electronics offers attractive properties including reduced overall system volume, reduction of high-current cabling, reduced radiated EMI, simplified cooling arrangements, and appealing fault tolerance opportunities.

However, physical integration of electric machines and drives presents many challenges. In order to integrate the controls and power electronics into the machine housing, the power electronics must be designed to operate reliably in elevated vibration and thermal environments that fall outside of standard ranges for industrial-grade components. Further complicating the challenges, customers for integrated drives typically expect the drive electronics to meet or exceed the lifetime of the machine, requiring very high reliability in demanding environments.

Early generations of integrated motor drives have typically used conventional three-phase induction or PM synchronous machines combined with standard voltage-source 6-switch bridge inverters to excite the machine. In many of these units, the drive is housed in its own enclosure

which, in turn, is mounted on the side or end of the machine. More aggressive concepts for integrated machine drives have been proposed that approach more closely the ultimate objective of mounting the complete drive inside the same enclosure as the machine, but commercialization of these advanced integrated drive architectures has been limited to date.

One of these advanced concepts that has been proposed in the literature is the integrated modular motor drive (IMMD) . As illustrated in Fig. 1.2, this concept segments the stator into individual pole pieces, each encircled by a concentrated winding that is excited by its own dedicated electronics unit that includes both the necessary power electronics and controls to form a complete pole-drive unit. The IMMD is completed by interconnecting a number of these pole-drive units to form an annulus around the rotor. Appealing features of this IMMD concept emerge from its modularity, offering opportunities for improved manufacturability, enhanced fault tolerance and redundancy, and simplified repair/replacement of the pole-drive units.

1.1 Motivation

Reliability and Redundancy

As electric drive systems move into many power and actuation applications previously handled by mechanical and hydraulic systems, reliability and redundancy becomes an important consideration for an electric drive.

In aerospace systems, a typical fault mitigation method is to use parallel actuators which are torque summed in order that a failed actuator does not cause system failure [1]. While this method is well understood and robust, it requires significant extra weight, volume, and cost over a single actuator able to perform the same task.

Argile et al. [2] described a Markov model method for describing converter faults and calculating the total MTTF for a fault-tolerant con-

verter model which is able to continue operation even in the face of lost power conversion components. This paper shows clearly both the difficulties posed by the increased failure rates caused by increasing component counts and the opportunities afforded by fault tolerance when repair is possible.

EMI Containment

As electric drives spread into automotive and residential areas at high powers, EMI mitigation becomes a major design challenge.

1.2 Previous Research

Previous research into integrated modular motor drives can be split into three categories.

System Level Designs and Integrated Converters

The first category, system-level research includes investigations into controlling high phase-order machines and fault tolerant drives to achieve continued system operation in the presence of machine and drive component failures.

The first of these investigations was carried out with a load commutated thyristor based inverter and a 6-phase induction machine. In his research [3] T. M. Jahns achieved full torque operation of a faulted machine with only minimal increase in machine and drive losses though the modification of applied voltage magnitude and frequency to the remaining healthy phases.

More recent related research has been undertaken at WEMPEC in the area of modular converter integration.

Recently Nate Brown and others [4] have demonstrated a fully modular machine consisting of tooth-wound SMC pole pieces coupled to a modularized inverter. The entire machine and drive are air cooled by drawing

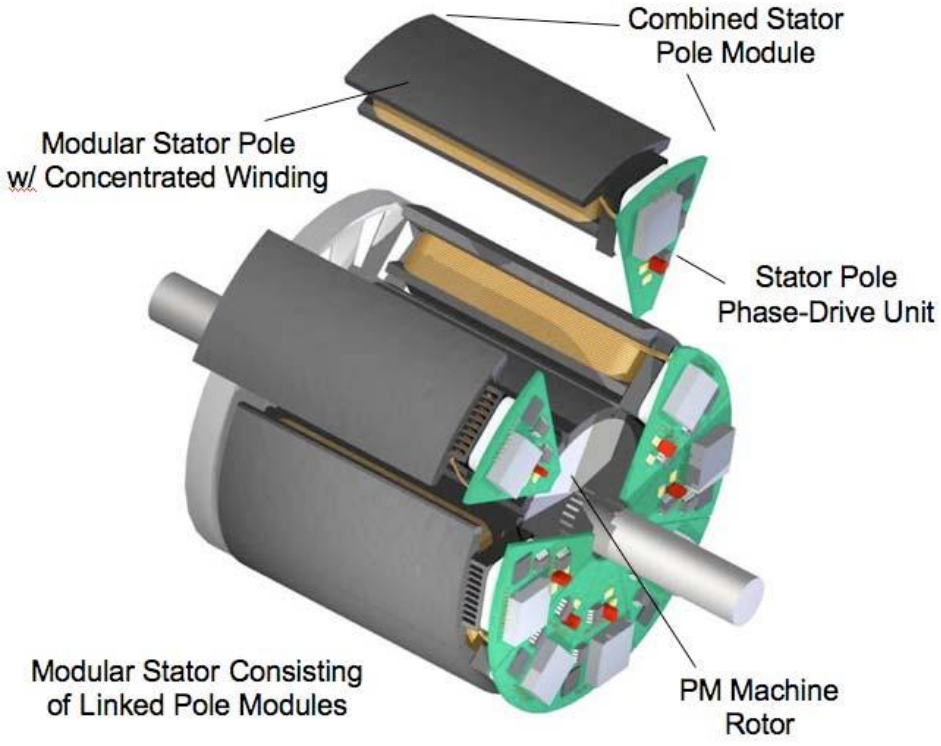

Figure 1.1: Rendered views of 5-phase SMC modular motor drive.

air first through the inverter poles then through the machine airgap and slots. The controls on this machine however are still fully centralized.

This modular inverter also demonstrated the difficulties in modular drive interconnect as its phase and power connections developed intermittent faults after a relatively short operating life.

Machine Design

The next category and a vital component of any motor control work is the design of the electric machine itself.

In order to allow easy redundancy and increased flexibility of operating with multiple phase configurations, this works focuses on a 6-phase machine with a 60 degree phase spacing. A dual winding 12 slot, 10 pole dual-layer design was chosen due to the highly isolated and contained flux paths [5]. This design allows for machine characterization and testing using standard 3 phase converters which greatly helps both in model design and system debugging.

Current Sensing

Accurate current sensing is a vital component of high-performance motor controls. Often this is accomplished through the use of transformer-based hall-effect sensors. Sadly, for an integrated application these sensors are both highly temperature sensitive and too large.

A much more compact current sensing method involves the use of free-space magnetic field sensors in fixed position relative to a current carrying conductor. This approach allows both small-size and high bandwidth as current sensor core materials do not come into play. In [6] GMR sensors are used as they allow for extremely large bandwidth (into the MHz range). These sensors are however unipolar and biasing magnet requirements offset some of the thermal stability gains.

Chapter 2

Abstract Design

2.1 Control Topology

While the controls topology is not a primary focus of this thesis, it is an essential driver of the converter design.

The starting requirements in the controls design for this project was to eliminate as many single-points of failure as possible using a separate controller per-phase.

This approach immediately drives a few control topology decisions. First, typical AC drive algorithms require knowledge of the complete state of the machine in order to generate commands. This would either necessitate either a very fast and tightly coupled communication structure or some method to decouple the controls from some of the machine states. As we are using a machine with 6 phases to allow for fault tolerance, broadcasting current sensor information each cycle would already overwhelm a typical CAN network. To avoid this problem we use the dual-wye connection of the drive and have each phase module sense only 3 currents: Its own, one on the same wye, and one on the opposite wye. Standard 3-phase drives already use a variant of this method by only sensing two currents for control. This allows a single phase controller to have a full

view of the currents in its wye while monitoring the other wye for faults.

By symmetry, running an identical control algorithm for each phase and picking the correct voltage output will allow standard vector control concepts to be used with minimal overhead. The variations in input sensors however will need to be corrected for and some effort will be required to achieve good power balance between phases.

Position sensing is also a problem and presents a single-point failure mechanism. For this work we are simply using a standard position sensor though standard resolver concepts can be extended to allow for each phase module to have its own resolver stator while using the same rotor.

For this work, we will be staring with V/Hz control as this is relatively robust and easy to implement with limited feedback required.

Non-synchronized PWM

While control states may be managed between modular drive processors with only moderate difficulty, the classical assumption that all PWM carriers are synchronized presents significant difficulty as a delay of only a few microseconds represents a significant phase delay. Thankfully, at normal carrier to fundamental ratios, the phase of the PWM carrier is unimportant to a first order as the machine inductance filters out the high frequency switching components. Quartz crystal-based main oscillators are quite stable and allow frequency tolerance below 100ppm without any special calibration. For a 20kHz PWM system, the beat frequency between PWM carriers will be at a frequency of 2Hz. This beat frequency will manifest as a peaking of the $\frac{dV}{dt}$ applied to the machine windings relative to the frame every 0.5s or longer depending on the specific spread of oscillator frequencies. While this phenomenon has little effect on the control of the machine, the effects on bearing currents and insulation lifetime have not been investigated.

Fault Management

A detailed consideration of fault management has been reserved for future work, but

2.2 DC-Link Design

DC-link design is a topic that is often overlooked in converter design. Usually it is relegated to rules-of-thumb which are often based on sound reasoning, but typically end up being used in situations where the assumptions they are based on do not hold.

The first of these rules is to size DC-Link capacitors based on a certain capacity per Watt of converter power rating. This rule is extremely easy to apply, but is typically based on the assumption of DC-Link currents being dominated by the 120Hz or 180Hz current ripple of a single-phase or 6-pulse diode rectifier. This rule also is specific to one voltage level as the ripple current and thus capacitance requirement is decreased as the inverse of the DC-link voltage. If not driven by controls requirements on DC-link voltage variation, this rule also assumes specific current handling capabilities of the capacitor (Typically electrolytic).

The next common rule is to design based on an allowed voltage ripple. This rule is significantly more robust than the converter-power based rule above as it takes into account varying ripple current conditions. This rule is also often dictated by the controls design as control accuracy will suffer if the DC-Link voltage variation is not decoupled.

A final rule of thumb is to size the DC-link capacitance to be thermally rated for a ripple current that is a given fraction of the converter's rated output current (typically two thirds the RMS phase current for common 3-phase converters). This is a very robust rule in terms of managing component lifetime, but may cause excess DC-Link voltage ripple if polymer

film-based capacitors are used due to their excellent current handling capability even at low capacitance ratings.

The matter of the precise spectrum of DC-link current is treated well in [7] where the current from a switching converter is calculated by convolving the output current with the switching voltage waveform. This approach confirms the two-thirds sizing rule for conventional three-phase 2-level VSI converters and adds the insight of how specific frequency components are related between phases.

Fig. 2.2 shows how the RMS ripple current is effected by changes in both modulation index and the output power factor of a three-phase converter. This plot is delineated as a ratio of RMS phase current to RMS DC-link ripple. The worst-case is at approximately a 0.6 modulation index with unity power factor (either motoring or generating). This plot also clearly shows that it is the switches, not the DC-link capacitor that circulates energy when a converter is operating at low power factor.

The main takeaway from this is that the interconnect between phases should have lower impedance than the interconnect between any single phase and the DC-source in order to allow cancellation of modulation-referenced ripple while the capacitors must be sized to handle switching-referenced ripple.

These three rules all encapsulate both their driving assumptions the two actual drivers of DC-link design.

First, whatever design is chosen must be capable of handling ripple-related thermal loads. This is a function of both dielectric heating effects and joule losses in capacitors and inductors. As capacitor technology advances with improvements in film capacitors and upcoming dielectric materials such as glass, designs based on thermal capability will become more necessary.

Second, a DC-link structure is at its core an impedance matching component which must present a low impedance to the power converter's

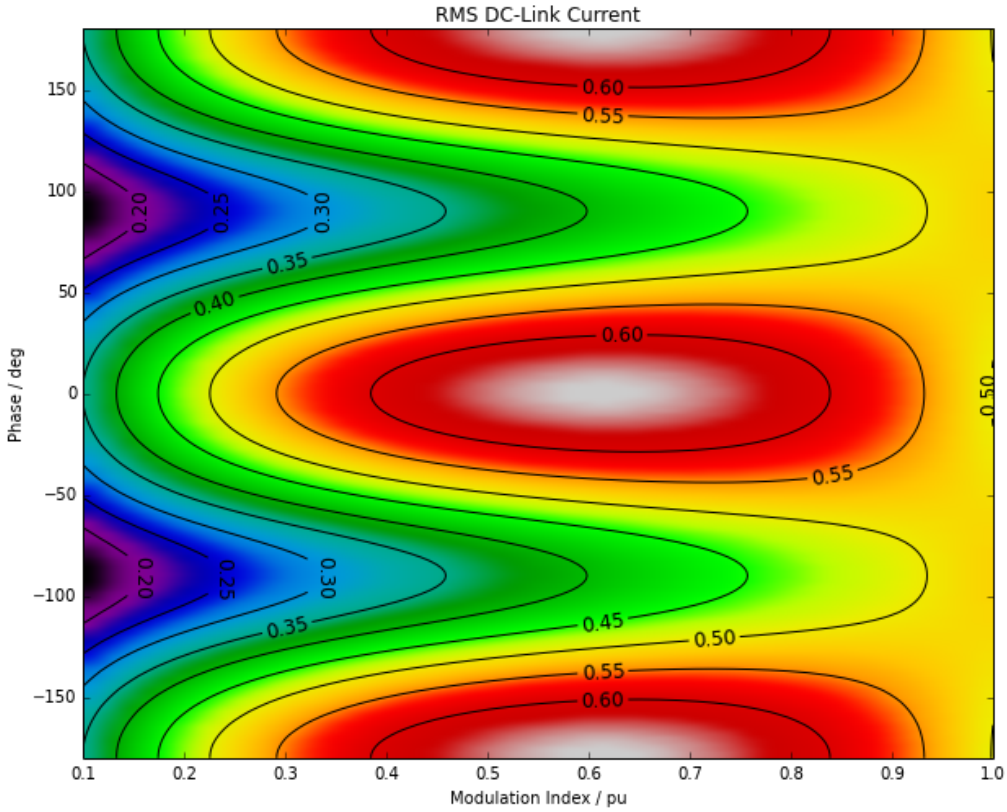

Figure 2.1: DC-link ripple current for a three-phase, two-level VSI operating without higher harmonic injection. Contour lines delineate ratio of RMS phase current to RMS ripple current.

switching pole at the switching frequency and higher, must present a low impedance at twice the power frequency due to reactive power handling requirements, and must present a high impedance at DC in order to ensure that bulk power flow comes from the power source.

While this is typically handled with bulk capacitance for standard VSI-based designs, the size and temperature constraints of the integrated modular motor drive require a more creative hybrid approach. An interesting aside is that resonant-link converters fully exploit this requirement to reduce switching losses and reactive component size.

Interconnect Design

For the integrated modular motor drive, we cannot tolerate the low temperature ratings of electrolytic capacitors. Because of this limitation, the total bulk capacitance available is much lower than would typically be used in a converter of this size. Furthermore, due to the distributed nature of the converter, reactive power currents must be passed through the DC-link structure to other modules before returning to the machine. In order to maintain an effective low impedance at the power frequency for reactive power while shielding these currents from the power source, a star-and-ring topology was chosen as described in previous work on IMMD power electronics.

While this ring-and-star approach is very effective at handling power-frequency harmonics, it does not keep a stiff DC-link at the switching frequency and higher. In order to accomplish this, I chose a frequency-splitting technique similar to what is used in high performance logic decoupling. To this end, the DC-link capacitance is split into three parts on each module: A bulk polyproylene film capacitor, a pair of multilayer ceramic capacitors, and an integrated PCB capacitor.

The overall DC-link layout is shown in Fig. 2.2.

Capacitor Sizing

Capacitor sizing was based entirely on current handling capability and size constraints. As power-frequency components are being primarily handled by the DC-Link interconnect we require little capacitance to manage reactive power flow. For the bulk DC-link capacitance, a 700V 20μF film capacitor from TDK was chosen as it can handle nearly the entire ripple current of a phase at rated load. This capacitor will be absorbing the kHz range ripple from the converter switching. The ceramic capacitors were chosen for high-voltage, low-inductance, and low dielectric loss. As these

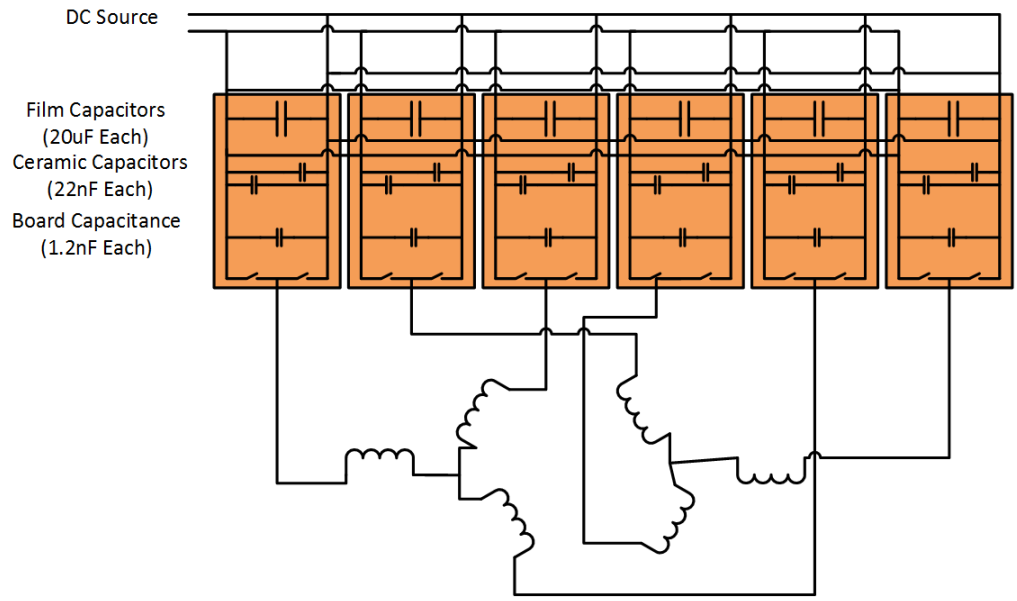

Figure 2.2: Schematic showing interconnection of power inverter and machine.

capacitors are placed directly on the DC terminals of the power modules, they will be handling the MHz range power frequencies caused by switching edges. Finally, the PCB itself was designed with nearly uniterrupted power planes which provided each board with 1nF of somewhat lossy capacitance at very low inductance which ensured that >10MHz ripple would not be injected into the other capacitors.

This multi-layer design allowed for low impedance with reduced overall capacitor size as is shown in the results section.

2.3 Peak Ratings

Electric machine and drive system ratings are influenced by a variety of factors. While continuous ratings for rated operating conditions are well defined and easily modeled and tested, peak ratings are dependent on

definitions. The determination of peak ratings is further complicated by marketing influences in that a large "peak power" number is an easily quoted figure of merit even if it has little real-world backing.

The peak rating of an electric drive system is driven by a number of factors depending on the peak time required. For peak times on the order of one electrical cycle, the power limit is driven by the saturation current allowed by the power switches and the demagnetization limit of the permanent magnets in the electric machine. Both of these limits are effected by the starting temperature of the electrical drive system, but are largely independent of other thermal effects as the peak time is too short.

For the FreedomCar/USDrive specification, peak power rating is defined as an 83% overload for 18 seconds. This overload time is of the same order as machine thermal time constants. From a converter sizing standpoint, this overload rating requires that the power switches are capable of handling the full overload power as they have sub-second thermal time consents. The remainder of the converter design however only needs to be rated to the continuous load as capacitor and interconnect thermal time constants are measured in minutes or longer. The cooling system for the power converter must be able to handle approximately the same overload as the machine as the extra cooling load from the power semiconductors will increase in proportion to output power. Finally, sensing must be able to accommodate the full overload if control is to be maintained during overloaded conditions.

Chapter 3

Detailed Design

In this chapter I describe in detail the design of the modular motor drive modules and system. In the sections that follow, the specific design choices and design drivers are outlined and schematic sections are presented. Overall drive component schematics and PCB layouts are contained in Appendix **??**.

3.1 Mechanical Layout

An important part of any integrated converter design is the mechanical layout and packaging or as some would say: "multiphysics integration". For this integrated modular drive design, the converter and all its controls will be mounted on the end of a 6-phase machine designed at 1/3 scale but full diameter for the FreedomCar/USDrive specification. This layout is shown in rendered view in Fig. 3.1

In order to shield the drive from EMI and fringing fields from the machine, the drive is mounted on a stainless steel baseplate of the same footprint as the stator. The drive consists of six phase drive modules which mount over the corresponding two stator tooth section of the machine. Each module is one sixth of the stator circumference. In order to allow easy

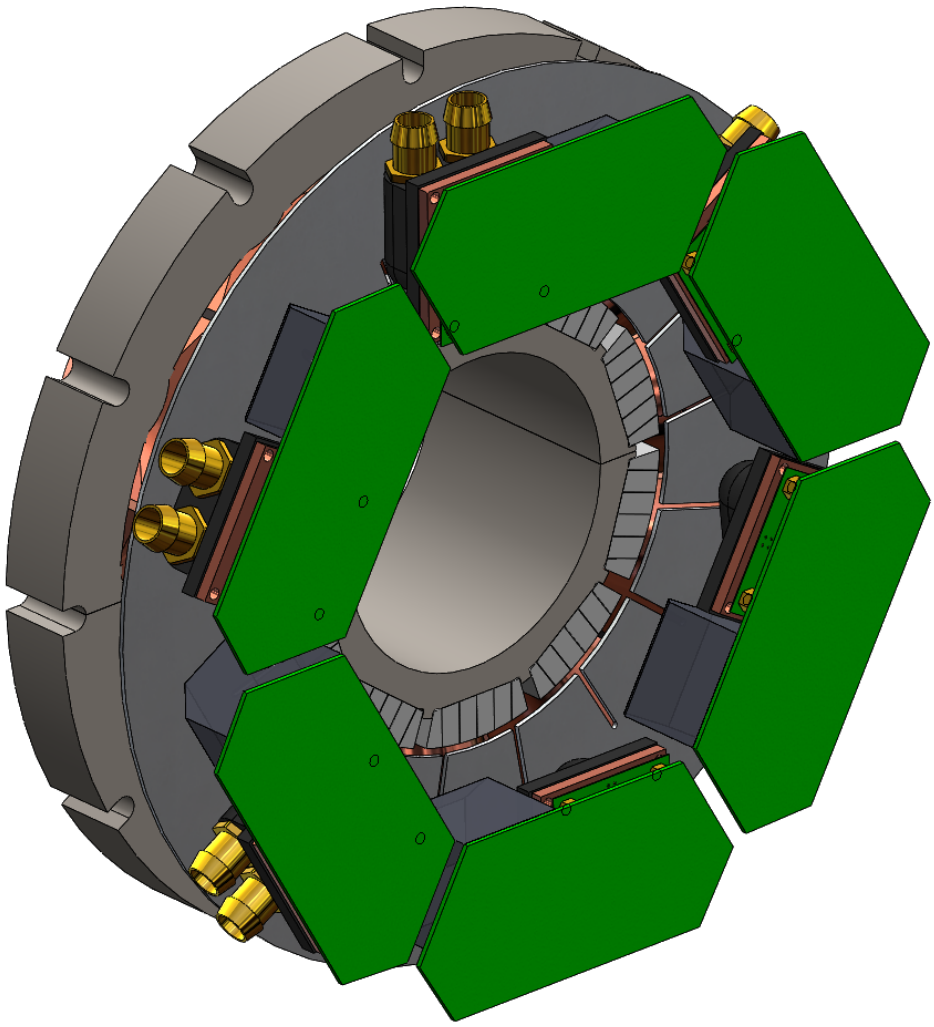

Figure 3.1: Rendered view of modular drive on machine.

fabrication each module consists of two printed circuit boards with bolt together interconnects which both allows for low-resistance connection for high-current paths and the ability to quickly change out damaged modules in case of faults.

Cooling is designed to be possible with either water or air. In this case water cooling is used as the machine is already cooled with a water jacket. The drive modules plumbed in series, upstream of the machine cooling water jacket.

3.2 Gate Drivers

Gate drive design for a tightly integrated motor drive is primarily driven by a need for small size and high output current. In this design, the DC-Link voltage is less than 600V which allows the use of commercial integrated bootstrap gate driver chips.

The FAN7390 integrated bootstrap gate driver was chosen as it supplies peak switching currents of more than 4 amps and handles undervoltage lockouts to ensure safe startup. This device is supplied in an 8 pin SOIC package and requires an external diode and bootstrap capacitor for high side supply. The temperature rating is for less than 150C junction temperature which requires less than 300mW of power dissipation in order to allow full temperature range operation in this design. Gate turn on and turn off is controlled through the use of a 10 Ohm turn on resistor with a turn off diode to help guard against shoot-through and ensure that Miller current injection cannot turn on the IGBTs.

Desaturation Detection

Power stage desaturation is measured on the low side by use of a diode clamped connection to the switching node tied to the 15V gate supply. This signal is then buffered by a P-channel MOSFET before being fed into a

digital input to the DSP as shown in figure 3.2. In the case of lower switch desaturation, this input will remain low which indicates to the software that a fault has occurred. In the case of high side desaturation, the fault can only be detected if the switching node voltage drops below 15V. This sensor can also detect shorted power switches within one switching cycle due to state mismatch with the gate drive commands.

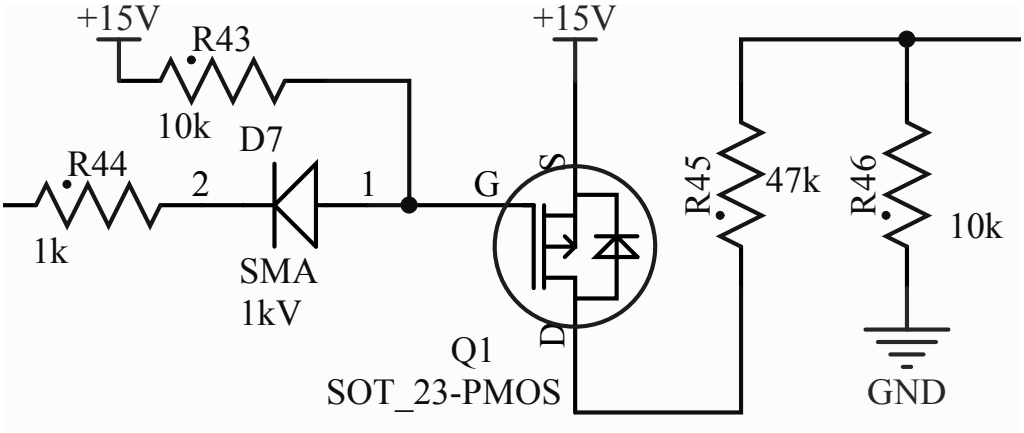

Figure 3.2: Schematic of desaturation detection circuit. Left end connects to switching node, right end to the DSP.

This method requires minimal hardware but will allow the controller to detect a blown switch withing one switching cycle so long as the DC link voltage is above 15V.

3.3 Power Module

While the power rating for this design is only 18kW, the system design was implemented with higher power ratings in mind. To this end, a small PCB was made to carry two discrete 600V IGBT-diode CoPacks, an RTC temperature sensor and a phase current busbar. This module mimics standard half-bridge IGBT modules from suppliers like Powerex

and Semikron at a smaller footprint and power rating more in line with the design goals of this system. The power module attaches to the control board by way of two bolt-down connections for the DC-Link and an 8 pin 100 mil header for gate connections and temperature sensing. The phase conductor busbar is used as part of the current sensing system described in the next section. This module is then strapped to the heatsink using a fiberglass clamp to cool the IGBTs. The design here allows for either air or water cooling though water cooling with a low cost video card water block was implemented during construction.

3.4 Current Sensing

Current sensing in this modular design was primarily driven by availability and ease of integration. While closed-loop sensors are most common for high performance motor drives, their requirement of encircling the phase conductor to be sensed meant that integration and easily disassembly would be difficult. Giant Magnetoresistive (GMR) sensors were also considered as they provide very small packages with excellent frequency response and dynamic range. GMR sensors however are more immature in the current sensing space and the unipolar nature of the sensor means that significant support is needed in terms of biasing and signal processing. The lack of a polished current sensing solution based on GMRs ruled them out of this design.

The current sensing design for the integrated modular motor drive was finally chosen to be an open-loop hall effect field sensor. The FHS 40-P device from LEM is a small SOIC-8 packaged device with minimal signal conditioning circuitry which is both low-cost and readily available. In order to use this device, it must be mounted on an area of PCB with an open aperture in the ground plane beneath it as is shown in figure 3.4. The current in a conductor mounted a fixed distance away is then sensed

by measuring the magnetic field impinging on the sensor.

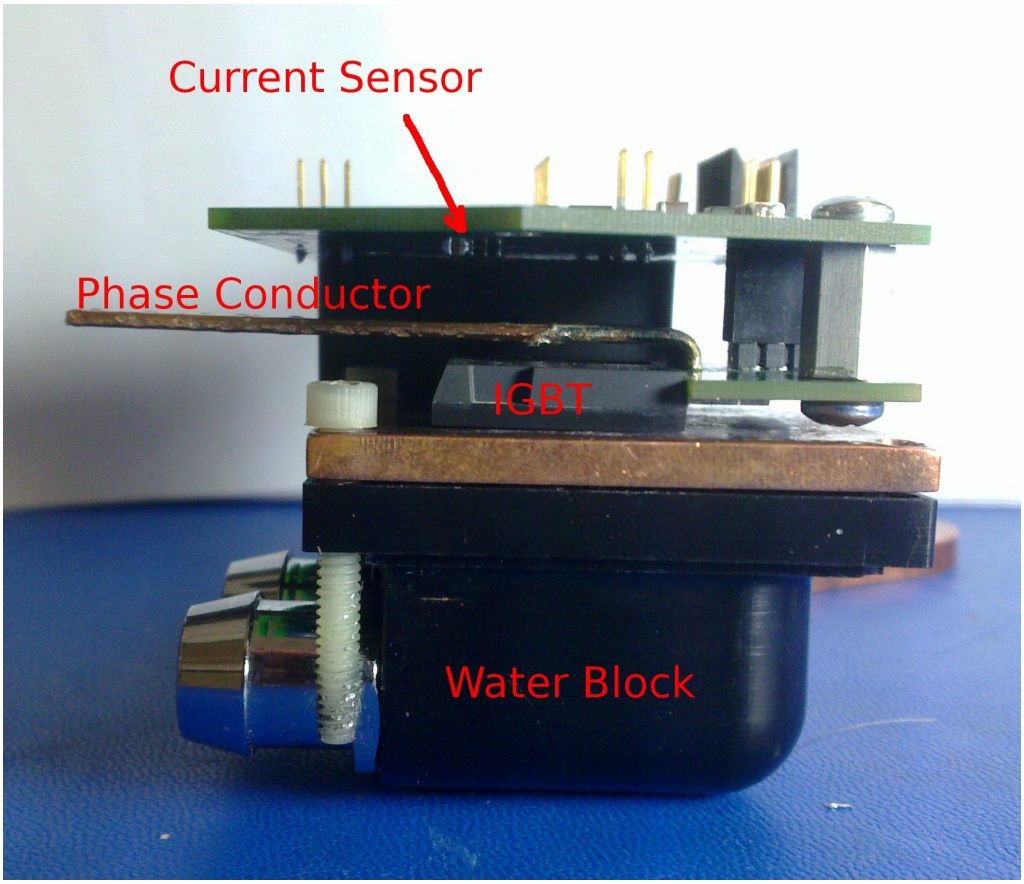

Figure 3.3: Side view of modular converter phase showing current sensor, waterblock, and phase conductor layout.

The spacing between the sensor and current carrying conductor is managed by the bolt-together standoffs between the controller board and the power semiconductor module.

Using a free-space field sensor in an application tightly integrated with an electric machine presents special challenges which were only exacerbated by the rotor in this machine being three times the length of the stator. In order to ensure current sensing was not contaminated

by offsets and noise from the machine below, the baseplate was chosen of a semi-ferromagnetic material (304 Stainless Steel) in order to shield low-frequency magnetic fields from the sensor. The copper faceplate of the water block directly below the power semiconductor module adds a further layer of shielding, using eddy currents to block higher frequency interfering fields from the sensor.

3.5 DSP

DSP selection for this converter was primarily driven by thermal considerations. In to allow the possibility of operating with incoming coolant at 105C, the processor needed to be able to operate at 125C or greater ambient temperatures.

At the time of design the only two options readily available were TMS320-series aerospace grade 200C processors from Texas Instruments or 140C rated dsPIC processors from Microchip. As this application requires approximately the same processing power as a standard three phase motor controller, the motor control dsPIC series processor is more than adequate.

A benefit of this DSP is that it is available in a QFN package which is extremely helpful for the tight packaging requirements of this design. Furthermore, the Microchip DSP costs an order of magnitude less than the Texas Instruments part primarily due to it's roots in automotive and industrial controls rather than military and aerospace applications.

3.6 Communications

Inter-module communications is one of most important variables in an integrated modular motor drive design. The minimum or optimal values for for intermodule communication are an item for future work. For this design, a combination of digital and analog communication was chosen.

In order to allow reasonable sensing of the current vector, each module receives an analog current signal from two other modules. One is another phase on the same star-connection in order to allow calculation of the complete current vector; the other is from an adjacent phase on the other star-connection which is used for fault-detection and monitoring. This connection was received through a differential amplifier with low-impedance termination possible if noise pickup becomes a problem. The schematic of this receive amplifier is shown in Fig. 3.6.

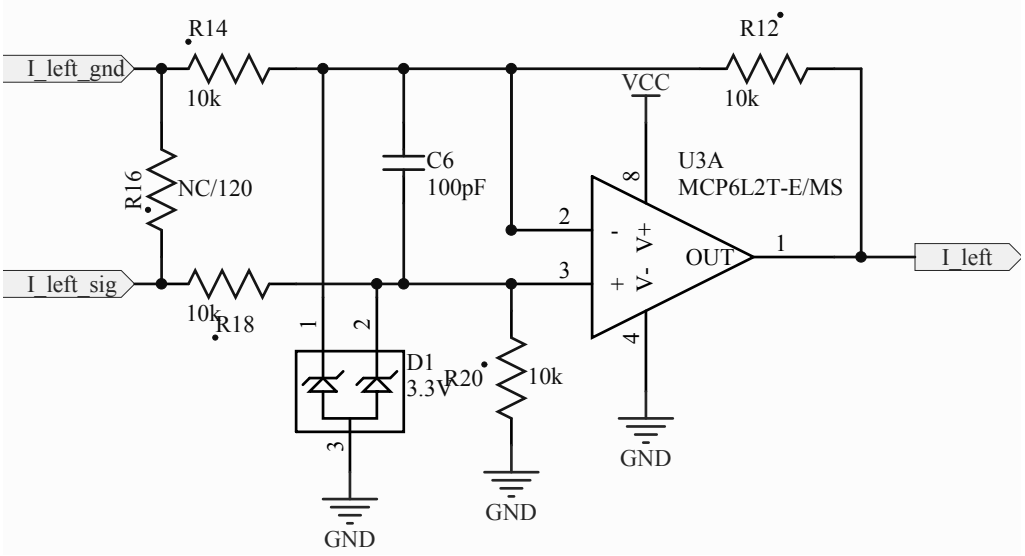

Figure 3.4: Left-adjacent current signal receive amplifier.

This analog communication is supplemented by a CAN bus operating at 1Mbps. This digital bus is used both for current vector command input and in order to share lower-bandwidth trimming values between modules.

Each module outputs it's measured values for the three currents which is read by the other modules and used to close the loop on sensor gain and offset in order to make the sensor input for control operation identical for all phases.

Chapter 4

Discussion

4.1 Hardware Performance

Controls development and hardware operation for this drive was severely hampered by a poor choice in inter-module connectors and lack of test-points. As such, full vector-control was never realized. Several important results however were able to be measured.

Current Sensors

The open-field hall effect current sensors on this prototype performed admirably both in providing nicely filtered signals and having interference from neighboring phases attenuated below what the system could measure.

The current sense amplitude response is shown in Fig. 4.1. This shows a roll off in amplitude above 1kHz. In a typical system this would be a problem due to phase lag, however this roll off is due to field shaping as the higher-frequency components of the magnetic field from the phase bar are concentrated near the edges of the phase conductor [6]. This gives the advantage that we can have switching frequency current components

attenuated while still having nearly lag-free response.

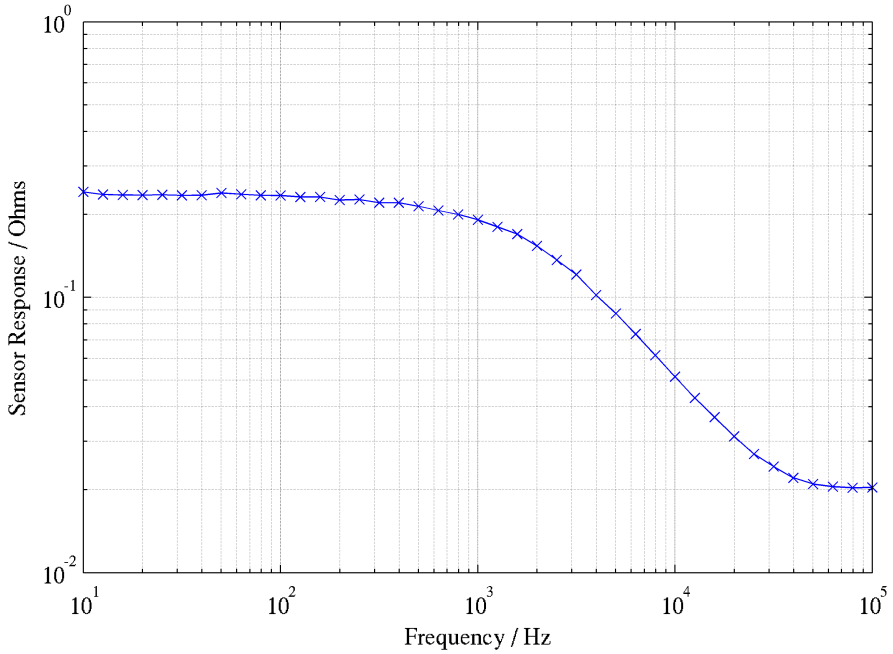

Figure 4.1: Current sensor gain response. Vertical units are ADC input voltage over phase current. The ADC operates on a 1.65V full scale.

Motor Operation

Due to cost, the motor used in this prototype has a 3x overlength rotor. This causes a significant increase in PM flux and brings the characteristic current to nearly 3pu. This machine decision was made after the converter was partially built and as such, the converter cannot survive fault transients at significant speed or full voltage.

The motor was thus operated at reduced voltage and brought up to just below its design corner speed of 2400rpm. Using V/Hz operation, the drive was able to run the machine smoothly operating with independent

control of all six phases. The waveforms for one phase are shown in Fig. 4.1.

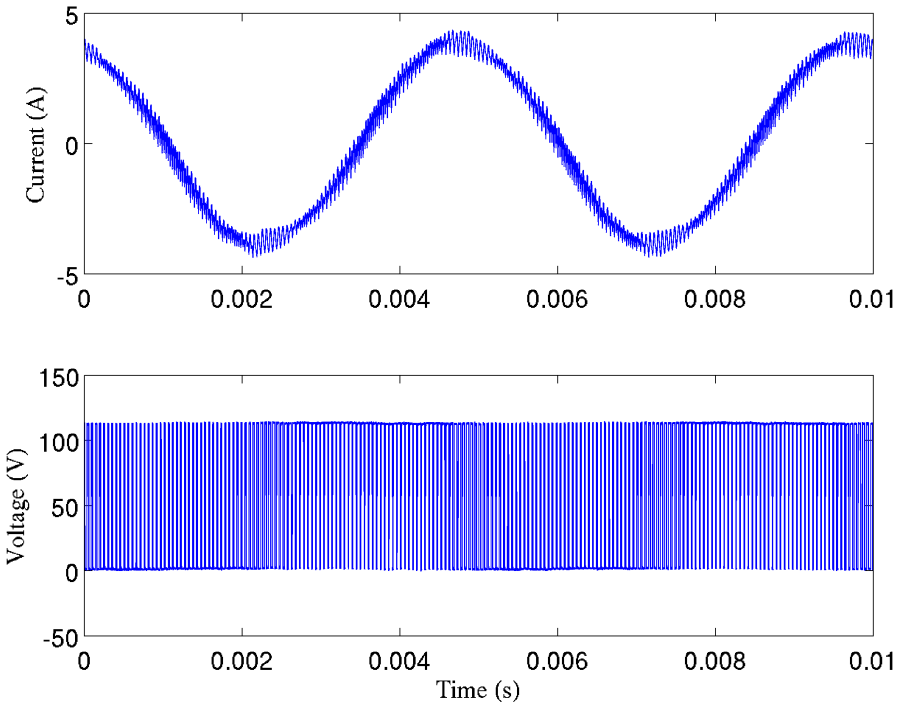

Figure 4.2: Waveforms for 2400rpm, V/Hz operation.

4.2 Scaling

A study was made of scaling the drive up to the full 55kW design required by the USDrive specification.

In that case, the only significant change would be a tripling of the capacitor size and a replacement of the power module component with a higher current device. Semikron and Infineon both supply 600V 300A modules in a similar footprint to the TO-247 based design used in this

prototype thus no further increase in volume is needed for the power switches. Our waterblock design also has significant cooling capacity overhead.

The capacitor resize would essentially double the size of the inverter as the current inverter volume is dominated by the waterblock and capacitor. Table **??** shows an overview of the volumetric and mass density of the prototype converter and upsized versions in both pancake arrangement where the drive covers the end of the machine rotor and annular where the drive footprint remains the same but the axial length is doubled.

Chapter 5

Conclusions

5.1 Contributions

This work has implemented a prototype hardware, tested current sensing with a free-field sensor, discovered issues with interconnect fragility, identified a path forward for controls development.

5.2 Future Work

Multi-phase IMMD

While the one phase per controller drive shown here provides significant gains in redundancy, multi-phase per controller modular designs show promise for simplifying the control of very large machines by allowing reduced converter complexity and wider application of commodity power switching components. Furthermore, having multiple phase voltages controlled by one controller significantly reduces the communications and coordination overhead in the system.

EMI analysis

Further work on EMI analysis is needed both in emission and susceptibility for tightly integrated motors and drives. This prototype implemented a few rules of thumb to allow the drive to operate, but there may be significant possible savings in weight and volume if the large baseplate can be eliminated. Furthermore, the savings in shielded cabling allowed by no longer having long motor phase leads with large dV/dt waveforms may make tightly integrated drives attractive to many applications.

Control Development

This work did not succeed in implementing high-bandwidth vector control. The most significant challenge is managing sensor tolerances in order to have all phases share power handling equally as independent controllers are not inherently symmetrical and can easily turn sensor errors into negative sequence components in the machine currents.

High-temperature Testing

This controller design was chosen with high temperature coolant in mind as multiple coolant loops are a significant overhead in current hybrid and electric vehicle designs. This design should be run at high temperature to determine where the actual thermal bottlenecks are so future designs can allow shared coolant between the drive and other system components.

Bibliography

[1] F. Annaz, "Monitoring in smart torque-summed actuators," in *Electrical Machines and Systems, 2009. ICEMS 2009. International Conference on*, Nov 2009, pp. 1–5.

[2] R. Argile, B. Mecrow, D. Atkinson, A. Jack, and P. Sangha, "Reliability analysis of fault tolerant drive topologies," in *Power Electronics, Machines and Drives, 2008. PEMD 2008. 4th IET Conference on*, April 2008, pp. 11–15.

[3] T. M. Jahns, "Improved reliability in solid-state drives for large asynchronous ac machines by means of multiple independent phase-drive units." Ph.D. dissertation, Massachusetts Institute of Technology, 1978. [Online]. Available: http://hdl.handle.net/1721.1/16184

[4] N. R. Brown, T. Jahns, and R. Lorenz, "Power converter design for an integrated modular motor drive," in *Industry Applications Conference, 2007. 42nd IAS Annual Meeting. Conference Record of the 2007 IEEE*, Sept 2007, pp. 1322–1328.

[5] N. Bianchi and S. Bolognani, "Fault -tolerant pm motors in automotive applications," in *Vehicle Power and Propulsion, 2005 IEEE Conference*, Sept 2005, pp. 747–755.

[6] P. Schneider, M. Horio, and R. Lorenz, "Integrating giant magneto-resistive (gmr) field detectors for high bandwidth current sensing in

power electronic modules," in *Energy Conversion Congress and Exposition (ECCE), 2010 IEEE*, Sept 2010, pp. 1260–1267.

[7] B. McGrath and D. Holmes, "A general analytical method for calculating inverter dc-link current harmonics," *Industry Applications, IEEE Transactions on*, vol. 45, no. 5, pp. 1851–1859, Sept 2009.